
Article:
Pintér, B. and Erdélyi, R. (2018) Fundamental (f) oscillations in a magnetically coupled solar interior-atmosphere system - An analytical approach. Advances in Space Research, 61 (2). pp. 759-776. ISSN 0273-1177

https://doi.org/10.1016/j.asr.2017.11.018

Fundamental (f) Oscillations in a Magnetically Coupled Solar Interior-Atmosphere System - An Analytical Approach

Balázs Pintér[1] and R. Erdélyi[2,3]

[1] *Institute of Mathematics, Physics and Computer Science, Aberystwyth University, Aberystwyth, UK, SY23 3BZ*
[2] *Solar Physics and Space Plasmas Research Centre (SP2RC), School of Mathematics and Statistics, University of Sheffield, Sheffield, UK, S3 7RH*
[3] *Department of Astronomy, Eötvös Loránd University, Budapest, P.O.Box 32, H-1518, Hungary*
[1] *Corresponding email: b.pinter@aber.ac.uk*

Abstract

Solar fundamental (f) acoustic mode oscillations are investigated analytically in a magnetohydrodynamic (MHD) model. The model consists of three layers in planar geometry, representing the solar interior, the magnetic atmosphere, and a transitional layer sandwiched between them. Since we focus on the fundamental mode here, we assume the plasma is incompressible. A horizontal, canopy-like, magnetic field is introduced to the atmosphere, in which degenerated slow MHD waves can exist. The global (f-mode) oscillations can couple to local atmospheric Alfvén waves, resulting, e.g., in a frequency shift of the oscillations. The dispersion relation of theglobal oscillation mode is derived, and is solved analytically for the thin-transitional layer approximation and for the weak-field approximation. Analytical formulae are also provided for the frequency shifts due to the presence of a thin transitional layer and a weak atmospheric magnetic field. The analytical results generally indicate that, compared to the fundamental value ($\omega = \sqrt{gk}$), the mode frequency is reduced by the presence of an atmosphere by a few per cent. A thin transitional layer reduces the eigen-frequencies further by about an additional hundred microhertz. Finally, a weak atmospheric magnetic field can slightly, by a few percent, increase the frequency of the eigen-mode. Stronger magnetic fields, however, can increase the f-mode frequency by even up to ten per cent, which cannot be seen in observed data. The presence of a magnetic atmosphere in the three-layer model also introduces non-permitted propagation windows in the frequency spectrum; here, f-mode oscillations cannot exist with certain values of the harmonic degree. The eigen-frequencies can be sensitive to the background physical parameters, such as an atmospheric density scale-height or the rate of the plasma density drop at the photosphere. Such information, if ever observed with high-resolution instrumentation and inverted, could help to gain further insight into solar magnetic structures by means of solar magneto-seismology, and could provide further insight into the role of magnetism in solar oscillations.

1. Introduction

The fundamental mode or f mode is a surface oscillation radially localised right beneath the solar photosphere in solar interior models (Christensen-Dalsgaard, 2002; Christensen-Dalsgaard et al., 2005). In plane-wave approximation with a free photosphere with no atmosphere above it in a standard solar model, the cyclic frequency of the f mode is $\nu = (2\pi)^{-1}\sqrt{gk}$. Here, g is the gravitational acceleration and k is the wavenumber of the oscillation mode, both taken at the photosphere. Measuring the f mode frequency is an effective diagnostic method for determining the near-photospheric physical features, like density or plasma flows. Among others, it also provides an accurate measure of the solar radius (Antia et al., 2000).

Observations show that helioseismic f and p (pressure) modes are effected by the presence of magnetic structures in the solar environment. By measuring the variations in properties of wave modes, we can probe the environment of the waves. This can be subsurface structures of magnetic active regions (Liang et al., 2013; Zhao & Chou 2016) or the lower atmospheric layers above the photosphere. Both inhomogeneities (e.g., density, temperature or magnetic) and dynamic changes (e.g., random or coherent flows) in the atmosphere can modify f and p mode properties (see e.g. Erdélyi et al., 2005; Mole et al., 2008; Kerekes et al., 2008,b). Frequencies (Libbrecht & Woodard, 1990; Chaplin et al., 2004; Dziembowski & Goode, 2005; Tripathy et al., 2006; Chaplin et al., 2007) and line widths (Tripathy et al., 2006; Lamb, 1932; Tripathy et al., 2006) of f and p oscillation modes vary in time and they correlate with the solar activity cycle (see also the review papers by Erdélyi, 2006a,b and Thompson, 2006). The observed magnetic effects on the helioseismic oscillations indicate that a possible connection between global f- and p-mode oscillations and the magnetic solar atmosphere. Solar atmospheric properties influence the helioseismic oscillations and as such the oscillation characteristics vary together with the variations of the atmospheric condition.

Our goal is to pursue this line of investigations by considering mathematically a coupled solar interior-atmosphere system as one single physical entity.

Considerable efforts have already been made to interpret the observed variations of the properties of global helioseismic modes. Possible effects of an atmospheric magnetic field on global solar oscillations were investigated first by Campbell & Roberts (1989) in a magnetohydrodynamic (MHD) model. In Cartesian geometry, they considered a two-layered model with a polytropic interior and an overlying atmosphere with constant temperature embedded in a horizontal magnetic field with constant Alfvén speed. They found that the magnetic field increases the frequency of the f mode. A series of other models followed that of Campbell & Roberts (1989). Various aspects of the global oscillations of the coupled solar interior and atmosphere were studied. Global waves propagating obliquely to the horizontal magnetic field have been investigated by Jefferies et al. (1990) and Pintér (2008). The effects of atmospheric temperature profiles have been studied by Vanlommel & Čadež (1998). Taroyan, Y. (2004) and Taroyan et al. (2004) have investigated effects of plasma flows on MHD waves. Random horizontal and vertical plasma flows both influence the f-mode properties (Mole et al., 2008; Kerekes et al., 2008b). Stochastic atmospheric magnetic fields are modelled by Erdélyi et al. (2005). In order to model the damping of global oscillations, the resonant coupling of these oscillations to atmospheric local slow and Alfvén waves was proposed and investigated in the context to contribute to the heating of the solar corona. This phenomenon is introduced in Sakurai et al. (1991), Zhukov (1997) and Tirry et al. (1998), and has been further explored by Pintér (1999), Pintér et al. (2007) and Taroyan & Erdélyi (2008,2008). Pintér & Erdélyi (2011) is an overview of modelling magnetic atmospheric effects on helioseismic oscillations.

In the present paper, we advance a coupled solar interior-atmosphere model in which magnetic atmospheric effects on f-mode frequencies due to the coupling of the interior to the atmosphere are studied in a three-layered model accounting for the interior, magnetic atmosphere and a transitional layer sandwiched in-between. An analytical form of the dispersion relation, $f(\omega, k) = 0$, is provided. The f-mode frequency is determined from the dispersion equation for two distinct cases. One considers an approximation with a solar interior and a single-layer magnetic atmosphere. In the other model, the magnetic field is turned off and a transitional layer is added to the lower part of the solar atmosphere representing e.g. the chromospheric canopy, in which the equilibrium parameters of the plasma vary continuously. Analytical formulae are derived for the frequency shift due to the presence of a thin transitional layer at the bottom of a magnetic atmosphere and, separately, due to the presence of a weak magnetic field in an atmosphere itself with a transitional layer.
All the earlier studies, e.g. those cited above, have used numerical methods to obtain a frequency versus wavenumber relationship, and their frequency spectra can only be presented graphically. The analytical approach in this study offers a clear complementary view of the influence of various plasma parameters, such as an atmospheric density scale-height, on the f-mode frequency. This may increase the diagnostic value of helioseismic observations as frequency shifts can be explicitly scaled with e.g. magnetisms or parameters determining stratification.

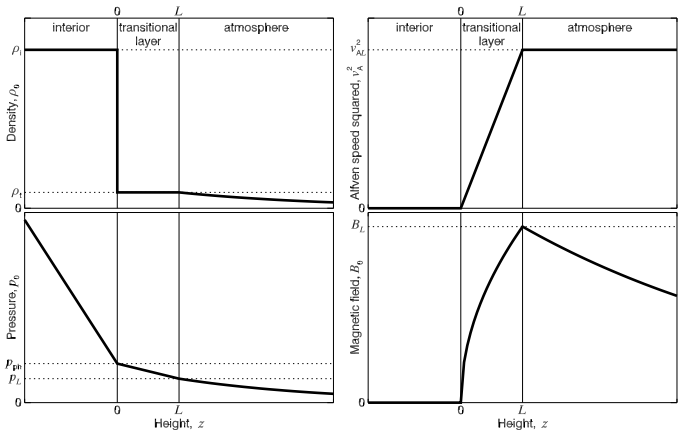

Figure 1: Equilibrium profiles for plasma density, $\rho_0(z)$, plasma pressure, $p_0(z)$, square of the Alfvén speed, $v_{\rm A}^2(z)$, and magnetic field strength, $B_0(z)$, in a plane-parallel three-layer solar model. In order to keep the generality of the model, no specific numerical scales are displayed along the axes. The physical meaning of the characteristic quantities $\rho_{\rm i}$, $\rho_{\rm t}$, $p_{\rm Ph}$, p_L, $v_{{\rm A}L}^2$, and B_L, indicated along the horizontal axes, is explained in the main text.

Our ultimate aim is to find, analytically, the consequences of resonant coupling between the solar interior and the inhomogeneous magnetised solar atmosphere. The study here is only the first step as we only focus on the incompressible mode of the interior-atmosphere system. We wish to shed light on the underlying physics before the complicated phenomenon of resonance is introduced in a follow-up study.

The simplified MHD model of the Sun is described in Section 2. A dispersion relation is derived analytically from the governing equations in Section 3. The dispersion relation is solved analytically for representative cases. The basic working model, described in Section 4, is a two-layer model with no magnetic field in the atmospheric layer. Next, a weak-field approximation is discussed in Section 5, where magnetism is introduced in the solar atmopshere, while Section 6 presents results of studies to obtain the frequencies of f-mode oscillations in a model with a thin transitional layer in the lower atmosphere, where the magnetic field strength increases continuously from zero with increasing height. We conclude in Section 7.

2. The Equilibrium

The Sun is modelled by a plane-parallel, three-layer plasma, using Cartesian geometry. One layer is the non-

magnetic solar interior. Above it is a magnetised transitional layer that is sandwiched between the interior and the magnetised overlaying atmosphere. The solar interior (atmosphere) can be defined by the optical depth being much larger (smaller) than one, $\tau >> 1$ [hidden] ($\tau << 1$ [visible]), respectively. The equilibrium values of all the physical quantities vary only vertically, with z. The helioseismic global oscillations are approximated in the plane-wave limit. The wavenumber of an oscillation mode is related to its harmonic degree as

$$k = \frac{\sqrt{l(l+1)}}{r},$$

where r is distance from the solar centre. For surface waves, $r \approx R_{\rm Sun}$. When the harmonic degree is much larger than one, $l >> 1$, the relationship between the wavenumber and harmonic degree of a wave mode simplifies to

$$l = kR_{\rm Sun}. \tag{1}$$

The curvature of the ray-paths of a propagating perturbation near the photosphere would be significant for oscillations with wavelengths comparable to the solar radius, $\lambda \left(\equiv \frac{2\pi}{k} \right) = R_{\rm Sun}$. This indicates that the plane-wave approximation is valid for f modes with $l \geq 7$. Due to this restriction, the model results have to be considered cautiously for low ($l < 10$) harmonic degrees.

Note that, in the standard solar model, with spherical geometry, the fundamental oscillation mode exists only with harmonic degrees above a threshold of $l \approx 20$.

The solar plasma is embedded in a vertical gravity field, $\vec{\mathbf{g}} = (0, 0, -g)$. The equilibrium plasma is static, that is, no flows are considered. The aim here is to study the f mode only, therefore, plasma perturbations are assumed to be incompressible indicating div$\vec{v} = 0$ and $\frac{d\rho}{dt} = 0$ (see Eq. 2).

Pressure (p) and gravity (g) oscillation modes will be the subject of a follow-up project. The MHD equations, a set of coupled partial differential equations, describe the temporal and spatial variations of plasma density, ρ, kinetic pressure, p, velocity, $\vec{\mathbf{v}}$ and magnetic induction, $\vec{\mathbf{B}}$. Of course, other variable representations may be chosen too. However, the above choice of primitive variables suits best and is most popular. A dispersion relation for the eigen-frequencies of the coupled interior-atmosphere system can be derived from the MHD equations. In this paper, we assume that dissipative forces are negligible. They play an important role, e.g., in resonant coupling between global helioseismic modes and local atmospheric MHD waves. Here, we use the ideal MHD equations that are the continuity equation (Eq. 2), the equation of momentum (Eq. 3), the energy equation (Eq. 4) and the induction equation with initial condition for the divergence of the magnetic induction (Eq. 5).

$$\left(\frac{\partial}{\partial t} + \vec{\mathbf{v}} \cdot \nabla \right) \rho = 0, \tag{2}$$

$$\rho \left(\frac{\partial}{\partial t} + \vec{\mathbf{v}} \cdot \nabla \right) \vec{\mathbf{v}} = -\nabla p + \frac{1}{\mu} (\nabla \times \vec{\mathbf{B}}) \times \vec{\mathbf{B}} + \vec{\mathbf{g}} \rho, \tag{3}$$

$$\left(\frac{\partial}{\partial t} + \vec{\mathbf{v}} \cdot \nabla \right) p = 0, \tag{4}$$

$$\frac{\partial \vec{\mathbf{B}}}{\partial t} = \nabla \times (\vec{\mathbf{v}} \times \vec{\mathbf{B}}), \qquad \nabla \cdot \vec{\mathbf{B}} = 0. \tag{5}$$

Perturbations occur around the following equilibrium. The solar non-magnetic interior in the model is a semi-infinite layer below the photosphere, $z < 0$, where the equilibrium density is constant, $\rho_0(z < 0) \equiv \rho_{\rm i}$. This indicates that the core of the Sun is artificially moved towards $z = -\infty$ in the model. Subscript 0 in the notation of physical quantities refers to their equilibrium values throughout the paper. The plasma pressure decreases linearly with height with a gradient $-g\rho_{\rm i}$. For gravity, the solar photospheric value is taken at $g = 274$ m s^{-2}, as the f mode, as a surface mode, concentrates near the photosphere.
The transitional layer is introduced in the simplest possible way, representing vertical inhomogeneity present in the solar atmosphere. Since the solar corona, by large, has large spatial scales, often of the order of tens of megametres (e.g., the gravitational scale-height is $\approx 50-100$ Mm), introducing a transitional layer may seem to be practical. The transitional layer may be viewed as a simple representation of the presence of the chromosphere. Of course, we have to be very careful not to over-interpret our findings, since this region is highly dynamic and inhomogeneous. Our main goal is to incorporate atmospheric magnetism. Hence, a horizontal magnetic field takes place above the photosphere, $z > 0$. This horizontal magnetic field may represent the presence of canopy-like structures in the lower atmosphere. Such chromospheric magnetic canopies have been observed by e.g. Giovanelli (1980). This approximation of the atmospheric magnetic structures is also supported by recent Hinode-observations that report ubiquitous granular-sized horizontal magnetic fields in the inter-network regions with field strengths around even a few hundred gauss, see Tsuneta et al. (2008), Lites et al. (2008), Ishikawa & Tsuneta (2010) and Ishikawa et al. (2010). Effects of vertical magnetic fields on magneto-acoustic waves, such as mode coupling and frequency shifts, in gravitationally stratified atmospheri models have been studied, for example, by Zhugzhda & Dzhalilov (1982), Cally & Bogdan (1993), Spruit & Bogdan (1992) and Hindman et al. (1996). Hindman et al. (1996) conclude that constant vertical magnetic fields can cause inefficient coupling of p oscillation modes to magnetohydrodynamic slow waves and the coupling results only in very small frequency shifts of the acoustic modes. F-modes, however, can couple strongly to vertical magnetic fields (Cally et al. 1994). Effects of tilted magnetic fields on wave propagation have been studied in MHD models by, e.g., Erdélyi et al. (2014)

and Mather & Erdélyi (2016).

In the lower part of the atmosphere, between $z \leq 0 \leq L$, the transitional layer is characterised as the square of the equilibrium magnetic field increases linearly from zero to its maximum, $B_L^2 \equiv B_0^2(z = L)$, thus the Alfvén speed squared in this layer, $v_{\rm A}^2(0 \leq z \leq L)$, also increases linearly. The Alfvén speed is defined as $v_{\rm A}(z) \equiv \dfrac{B_0(z)}{\sqrt{\mu\rho_0(z)}}$. L denotes the thickness of the transitional layer and $\mu = 4\pi \times 10^{-7}$ N A^{-2} is magnetic permeability. Note that this intermediate layer is not intended to model the so-called 'transition region' in the solar atmosphere.

The density has a discontinuity at $z = 0$ (i.e., at the solar surface) and it is constant in the transitional layer: $\rho_0(0 < z \leq L) = \rho_{\rm t} = \rho_{\rm i}/N$ with $N > 1$. This choice of model equilibrium is justified as the main point here is to introduce *magnetic* stratification, i.e., varying Alfvén speed. At this stage, it is less critical whether this is achieved by a constant density and varying magnetic field or vice-verse as our main point is to investigate whether global modes can couple to the atmosphere. The total pressure, the sum of the plasma (or kinetic) and magnetic pressures,

$$P(z) \equiv p(z) + \frac{B(z)^2}{2\mu}, \tag{6}$$

decreases linearly with a gradient $-g\rho_{\rm t}$.

The upper semi-infinite, i.e. third, layer models the solar atmosphere, where the Alfvén speed is constant, and the magnetic field strength and plasma density decrease exponentially with height. This layer is an approximation of the corona. Here the plasma pressure also tends to zero towards the outer atmosphere or the outer corona. We assume no plasma flows in the equilibrium: $v_0 = 0$. Hence, the equilibrium density, plasma pressure, magnetic field strength and Alfvén speed squared are determined by the following functions of height:

$$\rho_0(z) = \begin{cases} \rho_{\rm i}, & z < 0, \\ \rho_{\rm t}, & 0 \leq z \leq L, \\ \rho_{\rm t} \exp\left(\dfrac{L-z}{H}\right), & L \leq z, \end{cases} \tag{7}$$

$$p_0(z) = \begin{cases} p_{\rm Ph} - g\rho_{\rm i} z, & z < 0, \\ p_{\rm Ph} - \left(g + \dfrac{v_{\rm AL}^2}{2L}\right)\rho_{\rm t} z, & 0 \leq z \leq L, \\ p_L + gH\rho_{\rm t}\left(\exp\left(\dfrac{L-z}{H}\right) - 1\right), & L \leq z, \end{cases} \tag{8}$$

$$B_0(z) = \begin{cases} 0, & z < 0, \\ \sqrt{\mu\rho_{\rm t} v_{\rm AL}^2 \dfrac{z}{L}}, & 0 \leq z \leq L, \\ \sqrt{\mu\rho_{\rm t}} v_{\rm AL} \exp\left(\dfrac{L-z}{2H}\right), & L \leq z, \end{cases} \tag{9}$$

$$v_{\rm A}^2(z) = \begin{cases} 0, & z < 0, \\ v_{\rm AL}^2 \dfrac{z}{L}, & 0 \leq z \leq L, \\ v_{\rm AL}^2, & L \leq z. \end{cases} \tag{10}$$

The photospheric equilibrium plasma pressure, $p_0(z = 0)$, is denoted by $p_{\rm Ph}$. The plasma temperature, which is eliminated from the equations, can be obtained from the ideal gas law,

$$T_0(z) = \frac{M}{k_{\rm B}} \frac{p_0(z)}{\rho_0(z)},$$

where M is the mean molecular mass of the plasma and $k_{\rm B} \approx 1.38 \times 10^{-23}$ J K^{-1} is the Boltzmann constant. The equilibrium plasma pressure at the top of the transitional layer is $p_L \equiv p_0(z = L) = p_{\rm Ph} - (gL + v_{\rm AL}^2/2)\rho_{\rm t}$. The Alfvén speed squared at the top of the transitional layer, $v_{\rm AL}^2 \equiv v_{\rm A}^2(z = L)$, is a measure of the atmospheric magnetic field strength. The atmospheric scale-height, taken at the top of the transitional layer, $z = L$, is set to be,

$$H = \frac{p_L}{g\rho_{\rm t}}. \tag{11}$$

Following from Eq. (11), the atmospheric plasma pressure tends to zero with increasing z. Eq. (11) can be satisfied by setting the pressure-density ratio:

$$\frac{p_{\rm Ph}}{\rho_{\rm t}} = \left(g\,(L + H) + \frac{v_{\rm AL}^2}{2}\right). \tag{12}$$

The three-layer solar model we implement is one-dimensional in the sense that the physical quantities of the equilibrium depend only on the vertical, z, coordinate. The initial profiles given by Equations (7) to (10) describe the equilibrium fully, from which a dispersion function for wave propagation can be derived once the system is linearly perturbed.

The equilibrium profiles in the three layers of the model are illustrated in Fig. 1 for plasma density, $\rho_0(z)$, plasma pressure, $p_0(z)$, the square of the Alfvén speed, $v_{\rm A}^2(z)$, and the magnetic field strength, $B_0(z)$. In order to keep the generality of the model, no specific numerical values are given along the axes in Fig. 1. Here, the inhomogeneity (i.e. the linear dependency, as a first approximation) of the key physical quantities are important (e.g. Alfvén speed). Note that, although the derivations and Fig. 1 use an average 'mass density', ρ, with dimension kg m^{-3}, this average mass density can be converted to number density, n, with dimension m^{-3}, by dividing ρ_0 by the molecular mass of the plasma: $n \equiv \rho_0 M^{-1}$.

3. MHD Equations Governing the Perturbations

3.1. Ideal MHD Equations

Around a static equilibrium, we consider small perturbations of the physical quantities from their equilibrium values: $f(z,t) \approx f_0(z) + f_1(z,t)$ with $|f_1| \ll |f_0|$. This is a reasonable assumption as, for example, variations of

the solar radius (few hundred meters at most) are much smaller than the radius (7×10^8m), and amplitudes of observed photospheric radial velocity oscillations are only about 1 m s^{-1} (Elsworth et al., 1995), which are small compared to the sound speed (~ 5 km s^{-1}).
After linearising the equations, the perturbed quantities can be Fourier decomposed with respect to the horizontal coordinates, x and y, as the equilibrium quantities vary only in the vertical direction. The temporal and the horizontal spatial dependencies of the perturbations can be described by functions of plasma waves:

$$f_1(x,y,z,t) = f_1(z;k_x,k_y,\omega)\exp(i(k_x x + k_y y - \omega t)). \quad (13)$$

The x-axis is chosen to be parallel to the horizontal magnetic field. The linearized MHD equations in the Fourier space for an incompressible plasma with a horizontal magnetic field, derived from Equations (2) to (5) are:

$$\begin{aligned}
&\rho_1 + \frac{d\rho_0}{dz}\xi_z = 0,\\
&\rho_0\omega^2\vec{\xi} = \nabla P_1 - \frac{1}{\mu}\frac{d\vec{\mathbf{B}}_0}{dz}B_{1z} - \frac{i}{\mu}(\vec{\mathbf{k}}.\vec{\mathbf{B}}_0)\vec{\mathbf{B}}_1 - \vec{\mathbf{g}}\rho_1,\\
&p_1 + \left(\vec{\xi}.\nabla\right)p_0 = 0,\\
&\vec{\mathbf{B}}_1 = i(\vec{\mathbf{k}}.\vec{\mathbf{B}}_0)\vec{\xi} - \frac{d\vec{\mathbf{B}}_0}{dz}\xi_z.
\end{aligned} \quad (14)$$

The horizontal wave vector is defined as $\vec{\mathbf{k}} = (k_x, k_y)$. The Eulerian total pressure perturbation is

$$P_1 \equiv p_1 + \frac{1}{2\mu}\vec{\mathbf{B}}_0(z)\vec{\mathbf{B}}_1$$

(compare to Eq. (6)). The index '1', indicating the linear terms in the Fourier space, will be omitted henceforth. The Lagrangian displacement vector, $\vec{\xi}$, of which the time derivative is equal to the plasma flow velocity is:

$$\vec{\mathbf{v}}(z;k_x,k_y,\omega) \equiv \frac{d\vec{\xi}}{dt} = -i\omega\vec{\xi}. \quad (15)$$

Eliminating all the perturbed quantities but the z component of the displacement vector, ξ_z, from the linearized MHD equations (14), the following second-order differential equation can be obtained:

$$\begin{aligned}
0 = {}& \rho_0(z)\left(\omega^2 - \omega_{\rm A}^2(z)\right)\frac{d^2\xi_z(z)}{dz^2}\\
&+ \left(\frac{d\rho_0(z)}{dz}\left(\omega^2 - \omega_{\rm A}^2(z)\right) - \rho_0(z)\frac{d\omega_{\rm A}^2(z)}{dz}\right)\frac{d\xi_z(z)}{dz}\\
&-k^2\left(\rho_0(z)\left(\omega^2 - \omega_{\rm A}^2(z)\right) + g\frac{d\rho_0(z)}{dz}\right)\xi_z(z).
\end{aligned} \quad (16)$$

The local Alfvén frequency, as function of height, z, is defined as

$$\omega_{\rm A}(z) \equiv \frac{\vec{\mathbf{k}}.\vec{\mathbf{B}}_0(z)}{\sqrt{\mu\rho_0(z)}} = k_x v_{\rm A}(z).$$

Equation (16) can be solved in each layer of the model, and the solutions can be connected by appropriate boundary conditions to eliminate the unknown constants of integration. This will also provide a dispersion relation governing the permitted wave propagations.

3.1.1. *Interior*

Using the equilibrium profile, Equations (7) to (10), of the field-free interior ($z < 0$) with constant density, $\rho_{\rm i}$, the governing equation (16) reduces to the differential equation of a harmonic oscillator:

$$\frac{d^2\xi(z)}{dz^2} - k^2\xi(z) = 0.$$

The general solution is $\xi_z(z) = \xi_{z,i1}\exp(kz) + \xi_{z,i2}\exp(-kz)$. The coefficient of the second term is zero, $\xi_{z,i2} = 0$, to satisfy $\lim_{z\to-\infty}\xi(z) = 0$, the condition that all perturbations tend to zero towards the solar centre. In other words, we do not study leaky waves here, which carry energy to infinity.

3.1.2. *Transitional Layer*

The density is constant, $\rho_{\rm t}$, while the Alfvén speed and the Alfvén frequency, increase with z in the transitional layer ($0 < z < L$), therefore, Equation (16) can be written as:

$$\zeta^2\frac{d^2\xi(\zeta)}{d\zeta^2} + \zeta\frac{d\xi(\zeta)}{d\zeta} - \zeta^2\xi(\zeta) = 0, \quad (17)$$

with $\zeta \equiv -k\left(z - \frac{\omega^2}{\omega_{\rm A}^2}L\right)$. When the z-dependence of the Alfvén frequency is omitted, $\omega_{\rm A}^2$ stands for the Alfvén frequency taken at the top of the transitional layer, $z = L$:

$$\omega_{\rm A}^2 \equiv k^2 v_{\rm AL}^2 = k^2 v_{\rm A}^2(z = L). \quad (18)$$

The general solution to Equation (17) is a linear combination of modified Bessel functions I_ν and K_ν with index $\nu = 0$ (Abramowitz & Stegun, 1970):

$$\xi(z) = \lambda_1 I_0\left(k\left(z_{\rm Ph} - z\right)\right) + \lambda_2 K_0\left(k\left(z_{\rm Ph} - z\right)\right), \quad (19)$$

with λ_1 and λ_2 integration constants and $z_{\rm Ph} \equiv \frac{\omega^2}{\omega_{\rm A}^2}L$.

3.1.3. *Upper Atmosphere*

The plasma density decreases exponentially with height, while the Alfvén speed is constant in the atmosphere ($z > L$). In such an equilibrium, Equation (16) becomes a second-order differential equation with constant coefficients:

$$\frac{d^2\xi_z(z)}{dz^2} - \frac{1}{H}\frac{d\xi(z)}{dz} - k^2\left(1 - \frac{g}{H\left(\omega^2 - \omega_{\rm A}^2\right)}\right)\xi(z) = 0. \quad (20)$$

The general solution to the above differential equation is a linear combination of exponential functions:

$$\xi_z(z) = \xi_{zL1}\exp\left(\frac{1-\kappa}{2H}z\right) + \xi_{zL2}\exp\left(\frac{1+\kappa}{2H}z\right), \quad (21)$$

with ξ_{zL1} and ξ_{zL2} integration constants,

$$\kappa \equiv \sqrt{\left(1+4k^2H^2\right)\frac{\omega^2-\omega_{\rm C}^2}{\omega^2-\omega_{\rm A}^2}}$$

and

$$\omega_{\rm C}^2 \equiv \omega_{\rm A}^2 + \frac{4kH}{1+4k^2H^2}\omega_{\rm G}^2, \qquad \omega_{\rm G}^2 \equiv gk. \tag{22}$$

The kinetic energy density of the wave, which is proportional to $\rho_0\xi^2$, tends to zero with increasing height. The equilibrium density decreases exponentially with the scale-height, H, hence, the integration constant ξ_{zL2} must be zero (i.e., mathematically, to remain in Sobolev space).

3.1.4. Radial (Vertical) Profile of Perturbations

Therefore, the vertical displacement profile throughout the internal, transitional and atmospheric layers is:

$$\xi_z(z) = \begin{cases} \xi_{z0}\exp(kz), & z \le 0, \\ \lambda_1 I_0\left(k\left(z_{\rm Ph}-z\right)\right) + \lambda_2 K_0\left(k\left(z_{\rm Ph}-z\right)\right), & 0 \le z \le L, \\ \xi_{zL}\exp\left(\dfrac{1-\kappa}{2H}(z-L)\right), & z \ge L. \end{cases} \tag{23}$$

The gradient of the vertical displacement is:

$$\frac{d\xi_z(z)}{dz} = \begin{cases} \xi_{z0}k\exp(kz), & z \le 0, \\ -\lambda_1 k I_1\left(k\left(z_{\rm Ph}-z\right)\right) + \lambda_2 k K_1\left(k\left(z_{\rm Ph}-z\right)\right), & 0 \le z \le L, \\ \xi_{zL}\dfrac{1-\kappa}{2H}\exp\left(\dfrac{1-\kappa}{2H}(z-L)\right), & z \ge L. \end{cases} \tag{24}$$

I_1 and K_1 are modified Bessel functions with index $\nu = 1$ (Abramowitz & Stegun, 1970).

The perturbation function depends on the frequency, ω, of a particular oscillation mode explicitly and also implicitly, through κ and $z_{\rm Ph}$. Profiles of other physical quantities can be obtained from the set of linearised MHD equations (14), from which they have been eliminated, as linear combinations of $\xi_z(z)$ and its derivative, $\dfrac{d\xi_z(z)}{dz}$. For future reference, the main profiles of the MHD variables are:

$$\begin{aligned}
\rho(z) &= -\frac{d\rho_0}{dz}\xi_z(z), \\
p(z) &= \frac{B_0(z)}{\mu}\frac{dB_0(z)}{dz}\xi_z(z) + \frac{\rho_0\omega^2}{k^2}\frac{d\xi_z(z)}{dz}, \\
\xi_x(z) &= \frac{ik_x}{k^2}\frac{d\xi_z(z)}{dz}, \\
\xi_y(z) &= \frac{ik_y}{k^2}\frac{d\xi_z(z)}{dz}, \\
B_x(z) &= -\frac{dB_0(z)}{dz}\xi_z(z) - \frac{\mu\rho_0\omega_{\rm A}^2(z)}{k^2B_0(z)}\frac{d\xi_z(z)}{dz}, \\
B_y(z) &= -\frac{\mu\rho_0 k_y\omega_{\rm A}^2(z)}{k^2k_xB_0}\frac{d\xi_z(z)}{dz}, \\
B_z(z) &= \left(ik_xB_0(z) - \frac{dB_0(z)}{dz}\right)\xi_z(z),
\end{aligned} \tag{25}$$

where $\xi_z(z)$ and $\dfrac{d\xi_z(z)}{dz}$ needs to be substituted from Equations (23) and (24).

3.1.5. Dispersion Relation

At the interfaces, at $z = 0$ and $z = L$, the solutions must satisfy the physical boundary conditions that the vertical component of the Eulerian displacement, $\vec{\xi}(z)$ and the Lagrangian perturbation of total pressure, $\delta P(z) \equiv P(z) - g\rho_0(z)\xi_z(z)$, are continuous functions of z. Using (23) and (24), the Eulerian perturbation of total pressure has the following profile:

$$P(z) = \begin{cases} \xi_{z0}\dfrac{\rho_{\rm i}}{k}\omega^2\exp(kz), & z \le 0, \\ \dfrac{\rho_{\rm i}}{N}\dfrac{\omega_{\rm A}^2}{kL}\left(z-z_{\rm Ph}\right) \\ \quad\times\left(\lambda_1 I_1\left(k\left(z_{\rm Ph}-z\right)\right) - \lambda_2 K_1\left(k\left(z_{\rm Ph}-z\right)\right)\right), & 0 \le z \le L, \\ \xi_{zL}\dfrac{\rho_{\rm i}(1-\kappa)\left(\omega^2-\omega_{\rm A}^2\right)}{2NHk^2}\exp\left(-\dfrac{1+\kappa}{2H}(z-L)\right), & z \ge L. \end{cases} \tag{26}$$

Eliminating the integration constants, ξ_{z0}, λ_1, λ_2 and ξ_{zL}, from Equations (23) and (26), by using the boundary conditions for ξ_z and δP at $z = 0$ and $z = L$, provides us an implicit dispersion equation, of which the eigen-values, ω, are the possible eigen-frequencies of the coupled solar interior-atmosphere model:

$$\begin{aligned}
&\left(\omega^2K_1^0 - \gamma^2K_0^0\right)\left(2kHI_1^L + (1-\kappa)I_0^L\right) \\
&= \left(\omega^2I_1^0 + \gamma^2I_0^0\right)\left(2kHK_1^L - (1-\kappa)K_0^L\right)
\end{aligned} \tag{27}$$

with

$$\gamma^2 \equiv \omega^2 - (N-1)\omega_{\rm G}^2 \tag{28}$$

and

$$\begin{aligned}
I_{0/1}^0 &\equiv I_{0/1}\left(k\left(z_{\rm Ph}-z\right)\right), \\
K_{0/1}^0 &\equiv K_{0/1}\left(k\left(z_{\rm Ph}-z\right)\right), \\
I_{0/1}^L &\equiv I_{0/1}\left(k\left(z_L-z\right)\right), \\
K_{0/1}^L &\equiv K_{0/1}\left(k\left(z_L-z\right)\right),
\end{aligned}$$

where $z_L \equiv \dfrac{\omega^2-\omega_{\rm A}^2}{\omega_{\rm A}^2}L$.

Once the dispersion relation (27) is solved for ω, the vertical displacement, $\xi_z(z)$ and its gradient, $\dfrac{d\xi_z(z)}{dz}$, can be found by means of Equations (23) and (24). The vertical profile of any other physical MHD quantity can then be expressed by $\xi(z)$ and $\dfrac{d\xi(z)}{dz}$ in Equations (25). Note that the perturbation functions are all determined subject to an arbitrary coefficient, for example ξ_{z0}, as, by using the boundary conditions at $z = 0$ and $z = L$, the integration constants λ_1, λ_2 and ξ_{zL} can be expressed by ξ_{z0}. This is because we consider a linear problem.

4. Field-Free Atmosphere - No Transitional Layer

Before studying global oscillations affected by a solar atmospheric environment embedded in a magnetic field and with a transitional layer above the photosphere, we briefly consider the properties of f-mode oscillations in a simpler model that has only an internal ($z \leq 0$) layer and a single atmospheric ($z \geq 0$) layer, $L = 0$, with no magnetic field in it, $B = 0$ (or $v_{AL} = 0$). This simplification is useful in order to understand what the new features are introduced by the transitional layer and/or atmospheric magnetic field and what are intrinsic of the basic model. The conditions $L = 0$ and $v_{AL} = 0$ reduce the dispersion relation, Equation (27), to:

$$(2NkH - 1)\left(\omega^2 - \omega_R^2\right) + \sqrt{\left(1 + 4k^2H^2\right)\omega^2\left(\omega^2 - \omega_C^2\right)} = 0, \tag{29}$$

where the characteristic frequency ω_R is defined by

$$\omega_R^2 \equiv \frac{2(N-1)kH}{2NkH - 1}\omega_G^2.$$

Note that in a field-free atmosphere, ω_C^2, defined by Equation (22), reduces to

$$\omega_C^2 = \frac{4kH}{1 + 4k^2H^2}\omega_G^2.$$

The expression under the square-root in the dispersion relation (29) cannot be negative, therefore, any physical solution must satisfy $\omega^2 \geq \omega_C^2$. Another restriction to the solutions is that the square-root is non-negative, hence, the first term in Eq. (29) cannot be positive. For $k < k_R \equiv \dfrac{1}{2NH}$, this condition is satisfied for any $\omega^2 > 0$. For $k > k_R$, the solutions must satisfy $\omega^2 \leq \omega_R^2$.

Equation (29) yields a quadratic equation for the eigenvalue ω^2:

$$\begin{aligned} 0 = &\left(\omega^2 - \omega_G^2\right) \\ &\times \left(\left((N-1)^2 kH - N\right)\omega^2 - \left(N^2 - 1\right)kH\omega_G^2\right). \end{aligned} \tag{30}$$

The two solutions of the above equation are

$$\omega_-^2 = \omega_G^2$$

and

$$\omega_+^2 = \frac{(N-1)^2 kH}{\left(N^2 - 1\right)kH - N}\omega_G^2.$$

Solution ω_-^2 satisfies the dispersion relation, given by Equation (29), for $k \leq k_{CR}$, where k_{CR} is a threshold value for the wavenumber:

$$k_{CR} \equiv \frac{1}{2H}. \tag{31}$$

Recall that ω_G is the fundamental frequency in a standard solar model with no atmosphere. This indicates that the model atmosphere does not have any pronounced effect on the f mode with a small wavenumber (or low harmonic degree).

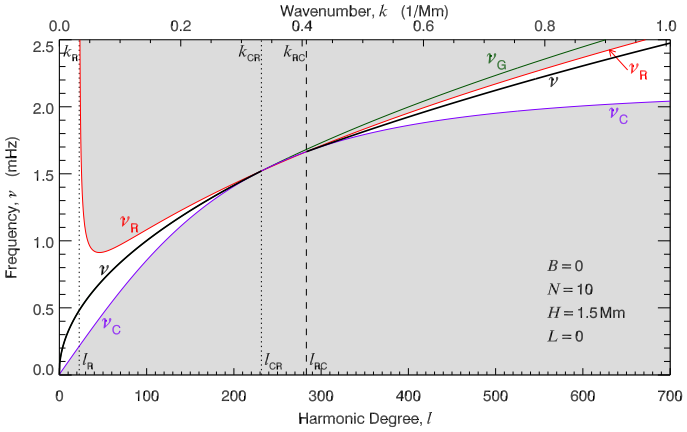

Figure 2: Frequency spectrum of the two-layer, $L = 0$, model with a field-free, $B = 0$, solar atmosphere for $N = 10$ and $H = 1.5$ Mm. The frequency of a fundamental (f) mode, ν, takes place between characteristic frequencies ν_C and ν_R. The f mode exists either with low, $l \leq l_{CR}$, or high, $l \geq l_{RC}$, harmonic degrees: they do not exist with harmonic degrees between l_{CR} and l_{RC}. The characteristic frequencies, ν_G, ν_C, and ν_R, harmonic degrees, l_R, l_{CR}, and l_{RC}, and wavelengths, k_R, k_{CR}, and k_{RC}, are defined in the main text.

The other solution of Equation (30), ω_+^2, satisfies the dispersion relation for $k \geq k_{RC}$, where k_{RC} is another threshold wavenumber:

$$k_{RC} \equiv \frac{N+1}{2(N-1)H}. \tag{32}$$

Using Eq. 1, the threshold wavenumbers can be converted to threshold harmonic degrees: $l_R = k_R R_{Sun}$, $l_{CR} = k_{CR} R_{Sun}$, and $l_{RC} = k_{RC} R_{Sun}$.
The solutions ω_- and ω_+ a called the low- and high-degree solutions.

With increasing wavenumber, k, ω_C exceeds ω_R at the smaller threshold, $k = k_{CR}$, while ω_R becomes larger than ω_C, again, at the larger threshold wavenumber, $k = k_{RC}$. Between k_{CR} and k_{RC}, where ω_C is larger than ω_R, neither of the solutions of Equation (30) satisfies the conditions $\omega_C^2 \geq \omega^2 \geq \omega_R^2$, therefore, no stable f mode can exist with wavenumber in the window $k_{CR} < k < k_{RC}$ (or with harmonic degree in the range $l_{CR} < l < l_{RC}$). Both solutions increase with increasing k, and ω_+ is below the fundamental frequency, ω_G, that is, the model atmosphere lowers the f-mode frequency in the high-degree range. With increasing wavenumber, the mode frequency tends to $\lim\limits_{k\to\infty} \omega_+ = \sqrt{\dfrac{N-1}{N+1}}\omega_G$.

The frequency spectrum of a typical field-free two-layer model is shown in Figure 2 for $l \leq 700$. The photospheric density drop is chosen to be $N = 10$. This value depends on where we draw the $z = 0$ hight in the real Sun. In Sections 5.2.1 and 6, we study the effects of a varying value for N. The atmospheric density scale-height is characterised by $H = 1.5$ Mm. The harmonic degree, l, and the associated wavenumber, k, are shown along the lower and upper horizontal axes, respectively. Although the derivations

have angular frequencies, ω, the results, such as eigen-frequency spectra and eigen-frequency shift profiles, will be displayed and discussed in terms of cyclic frequencies, $\nu \equiv \frac{\omega}{2\pi}$. This is because observations are given in the form of the latter more frequently.

The regions where no f-mode frequencies can occur, above $\nu_{\rm C}$ or below $\nu_{\rm R}$, are shaded grey. The dotted and dashed vertical lines indicate the three threshold values for k (and l).

The characteristic frequency $\nu_{\rm R}\left(\equiv \frac{\omega_{\rm R}}{2\pi}\right)$ is discontinuous at $k = k_{\rm B} \equiv \frac{1}{2NH}$, indicated by a vertical dotted line, as the denominator of $\nu_{\rm R}^2$, becomes zero for that value of $k = k_{\rm R}$. For the parameter values taken in Figure 2, $\nu_{\rm R}^2$ is negative for $k < k_{\rm R}$, hence, $\nu_{\rm R}$ is imaginary, and positive for $k > k_{\rm R}$.

In a two-layer model where the interior is modelled with a polytrope and the non-magnetic atmospheric layer is isothermal Campbell & Roberts (1989), the f mode is a surface wave with the fundamental frequency, $\omega = \omega_G\left(\equiv\sqrt{gk}\right)$. In that model, a stable f oscillation mode exists for the entire spectrum. A range of wavelength with no f modes appear only when the atmospheric layer becomes magnetic.

5. Weak-Field Approximation

Let us consider first a three-layer atmospheric model with a weak magnetic field in its atmosphere. A weak atmospheric magnetic field can be defined by the following conditions for the characteristic Alfvén speed:

$$v_{\rm A}L << \sqrt{gH}. \tag{33}$$

This assumption allows us to linearise the dispersion relation, Equation (27), with respect to $\omega_{\rm A}^2$, by which, the oscillatory behaviour of the model can then be investigated analytically.

$$\begin{aligned} 0 = &(1-\kappa_0)\left(\omega_0^2 C + \gamma^2 S\right) - 2kH\left(\omega_0^2 S + \gamma^2 C\right) \\ &+2\omega_0\Bigg(\left(1-\kappa_0\right)\left(C+NS\right) \\ &-\frac{2kH\left(\omega_0^2 C+\gamma^2 S\right)\omega_{\rm G}^2}{\kappa_0\omega^4}\Bigg)\Delta\omega \\ &-\left(\frac{(1-\kappa_0)S}{2kL} - \frac{2kHgk\left(\omega_0^2 C+\gamma^2 S\right)}{\kappa_0\omega^4}\right)\omega_{\rm A}^2, \end{aligned} \tag{34}$$

Here, ω_0^2 denotes eigen-frequencies of the three-layer model with field-free atmosphere; $S \equiv S$ and $C \equiv C$ are the sine hyperbolic and cosine hyperbolic functions of kL; and

$$\kappa_0 = \sqrt{\left(1+4k^2H^2\right)\frac{\omega_0^2-\omega_{\rm C}^2}{\omega_0^2}}.$$

5.1. Analytical Solutions to the Field-Free Model

The linearised dispersion relation (34) can now be separated to leading terms, containing neither $\Delta\omega$ nor $\omega_{\rm A}^2$, and first order terms. The leading terms provide the dispersion relation of the model with a field-free ($B = 0$) atmosphere:

$$2kH\left(\omega_0^2 S + \gamma^2 C\right) = \left(1-\kappa_0\right) \times \left(\omega_0^2 C + \gamma^2 S\right), \tag{35}$$

Using the definition of γ^2, given by Eq. (28), Equation (35) can be written in the following form:

$$R\omega_0^2\left(\omega_0^2-\omega_{\rm R}^2\right) = E\left(\omega_0^2-\omega_{\rm E}^2\right)\sqrt{\left(1+4k^2H^2\right)\omega_0^2\left(\omega_0^2-\omega_{\rm C}^2\right)}, \tag{36}$$

with

$$R \equiv (2NkH-1)\,C + (2kH-N)\,S, \tag{37}$$

$$E \equiv C + NS,$$

$$\omega_{\rm R}^2 \equiv (2kHC-S)\,\frac{N-1}{R}\omega_{\rm G}^2, \tag{38}$$

$$\omega_{\rm E}^2 \equiv S\frac{N-1}{E}\omega_{\rm G}^2. \tag{39}$$

The square of dispersion relation (36) is a cubic function of ω_0^2. Its three roots are:

$$\omega_{00}^2 = \omega_{\rm G}^2,$$

$$\omega_{\pm}^2 = \frac{\left(N^2-1\right)(S+C)\,S - (N-1)^2\left(kH \pm D\right)}{2NC_2 + \frac{N^2+1}{2}S_2 - 2\left(N^2-1\right)kH}\omega_{\rm G}^2,$$

with

$$D^2 \equiv \left((S-C)\,S + kH\right)^2 + \frac{4kH}{N-1}\left(S-C\right)S,$$

$$C_2 \equiv \mathrm{ch}(2kL), \qquad S_2 \equiv \mathrm{sh}(2kL).$$

The solutions ω_{00}^2, ω_+^2 and ω_-^2 are also roots of dispersion relation (36) only if

$$\omega_0^2 > \omega_{\rm C}^2 \tag{40}$$

and

$$R\left(\omega_0^2-\omega_{\rm R}^2\right)E\left(\omega_0^2-\omega_{\rm E}^2\right) > 0. \tag{41}$$

Such solutions are f-mode frequencies of the coupled solar interior-atmosphere model. The frequencies $\omega_{\rm C}$, $\omega_{\rm R}$ and $\omega_{\rm E}$, defined by Eq.s (22), (38) and (39), are interpreted as characteristic cut-off frequencies, which, in a frequency spectrum, separate regions of frequencies where real, physical solutions to the dispersion relation can or cannot occur.

The frequency spectrum for the field-free model for $l \leq 700$ is shown in Figure 3 for an $L = 2$ Mm thick transitional layer. This representative value is chosen to mimic the transition of the physical parameters between the photosphere and corona. The lower horizontal axis displays the harmonic degree, l. The related wavenumber, k, is also provided, along the upper horizontal axis, on the top of the panel. The solutions to dispersion relation,

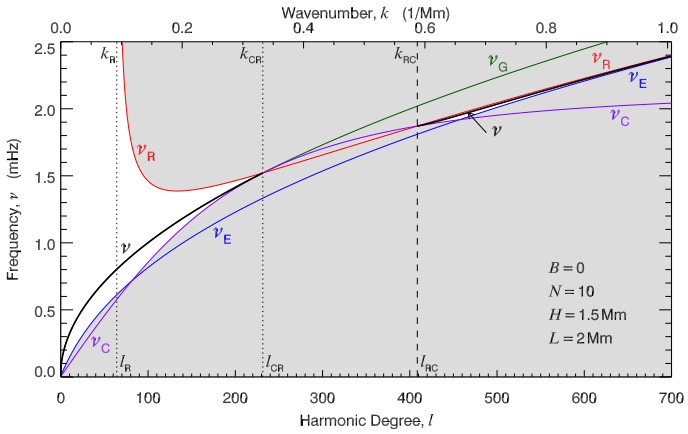

Figure 3: Frequency spectrum of the three-layer, $L = 2$ Mm, model with a field-free, $B = 0$, solar atmosphere with $N = 10$ and $H = 1.5$ Mm. The frequency of a fundamental (f) mode, ν, is lower than $\nu_{\rm R}$ and higher than $\nu_{\rm C}$ and $\nu_{\rm E}$. The f mode exists either with low, $l \leq l_{\rm CR}$, or high, $l \geq l_{\rm RC}$, harmonic degrees only. The characteristic frequencies, $\nu_{\rm G}$, $\nu_{\rm C}$, $\nu_{\rm E}$, and $\nu_{\rm R}$, harmonic degrees, $l_{\rm R}$, $l_{\rm CR}$, and $l_{\rm RC}$, and wavelengths, $k_{\rm R}$, $k_{\rm CR}$, and $k_{\rm RC}$, are defined in the main text.

Equation (36), in terms of cyclic frequencies, $\nu \left(\equiv \dfrac{\omega}{2\pi}\right)$, are:

$$\begin{aligned} \nu_{00}^2 &= \nu_{\rm G}^2, \\ \nu_{\pm}^2 &= \frac{(N^2-1)\,(S+C)\,S - (N-1)^2\,(kH \pm D)}{2NC_2 + (N^2+1)\,S_2 - 2\,(N^2-1)\,kH}\nu_{\rm G}^2, \end{aligned} \tag{42}$$

where $\nu_{\rm G} \equiv \dfrac{\omega_{\rm G}}{2\pi}$.

In Figure 3, the atmospheric scale-height is $H = 1.5$ Mm, and the equilibrium density drops at $z = 0$ by a factor $N = 10$. The frequency regions where conditions (40) and (41) are not satisfied, are indicated by grey shading. The verticals at $k_{\rm R}$ and $k_{\rm RC}$ are dotted lines while $k_{\rm CR}$ is plotted as a dashed line.

Wavenumber $k = k_{\rm R}$ is the solution for $R(k) = 0$ (see Equation 37). At this value, the denominator in the definition for $\nu_{\rm R}^2$ becomes zero, which causes $\nu_{\rm R}^2$ to be singular. For values for N and H, $k_{\rm R}$ is a threshold value for $\nu_{\rm R}$, as $\nu_{\rm R}^2(k < k_{\rm R}) < 0$ and $\nu_{\rm R}^2(k > k_{\rm R}) > 0$. Therefore, $\nu_{\rm R}$ exists only for $k > k_{\rm R}$.

At $k = k_{\rm CR} \equiv \dfrac{1}{2H}$, the three characteristic frequencies $\nu_{\rm G}$, $\nu_{\rm R}$ and $\nu_{\rm C}$ are equal. In the low-l range of the spectrum, $k \leq k_{\rm CR}$, only $\nu = \nu_0$ satisfies conditions (40) and (41). The f-mode frequency there is larger than $\nu_{\rm E}$ and $\nu_{\rm C}$ and, for $k > k_{\rm R}$, lower than $\nu_{\rm R}$. Frequencies ν_+ and ν_- are not solutions to Equation (36) in the low-l (or small-k) domain as ν_+^2 is negative and ν_- is lower than $\nu_{\rm C}$ for $k \leq k_{\rm RC}$.

Characteristic frequencies $\nu_{\rm R}$ and $\nu_{\rm C}$ become also equal at $k = k_{\rm RC}$. In the range $k_{\rm CR} < k < k_{\rm RC}$, $\nu_{\rm C}$ is larger than $\nu_{\rm R}$, which results in no permitted frequency range to satisfy conditions (40) and (41). In this intermediate range of l (or k), no f mode can exist.

In the high-l range of the spectrum, $k \geq k_{\rm RC}$, there is a frequency interval above $\nu_{\rm C}$ and $\nu_{\rm E}$ and below $\nu_{\rm R}$, where conditions (40) and (41) are satisfied. The width of the interval decreases with increasing k because the asymptots for $\nu_{\rm R}$ and $\nu_{\rm E} (> \nu_{\rm R})$ become equal:

$$\lim_{k\to\infty} \nu_{\rm R} = \lim_{k\to\infty} \nu_{\rm E} = \frac{N-1}{N+1}\nu_{\rm G}. \tag{43}$$

For $k \geq k_{\rm RC}$, frequency ν_0 ande ν_+ are larger than $\nu_{\rm R}$, therefore, they are no valid solutions to Equation (36). Frequency ν_-, however, lies in the narrow region above $\nu_{\rm C}$ and $\nu_{\rm E}$ and below $\nu_{\rm R}$, hence the f-mode frequency for the high-l range is $\nu = \nu_-$. It can be seen from Equations (42) that $\nu_-\,(k = k_{\rm RC}) = \nu_{\rm C} (= \nu_{\rm R})$ and

$$\lim_{k\to\infty} \nu_- = \frac{N-1}{N+1}\nu_{\rm G},$$

therefore, the f-mode frequency in the model with a field-free atmosphere is:

$$\nu_0 = \begin{cases} \nu_{\rm G}, & k \leq k_{\rm CR} \\ \nu_-, & k \geq k_{\rm RC}. \end{cases} \tag{44}$$

Henceforth in Section 5, ν_0 and ω_0 ($\equiv 2\pi\nu_0$) will denote the cyclic and angular f-mode frequencies, respectively, either in the low- or high-degree range, as given by Equation (44).

5.2. Analytical Solutions to Weak-Field Approximation

The presence of a magnetic field in the solar atmosphere modifies the eigen-frequency of the f mode:

$$\omega = \omega_0 + \Delta\omega, \tag{45}$$

where ω_0 denotes the oscillation frequency for a field-free model, while $\Delta\omega$ is the shift due to the presence of magnetic field. A weak magnetic field, defined by Equation (33), results in a frequency shift small compared to the field-free frequency value:

$$\Delta\omega << \omega_0. \tag{46}$$

Equation (36), the leading terms of the linearised dispersion relation (34), provide the f-mode frequencies of a model with a field-free atmosphere, given by Equation (44), as introduced in Section 5.1. The first-order terms of Eq. (34), on the other hand, determine the linear relationship between the square of the characteristic Alfvén frequency, $\omega_{\rm A}^2$, and the resulting frequency shift, $\Delta\omega$:

$$\Delta\omega = \frac{\lambda_{\rm num}}{\lambda_{\rm den}}\frac{\omega_{\rm A}^2}{2\omega_0}, \tag{47}$$

where

$$\begin{aligned} \lambda_{\rm num} &= \left((2NkH + 1 - \kappa_0)\,\omega_0^2 - 2(N-1)kH\omega_{\rm G}^2\right)\frac{\kappa_0 S}{2kL}\omega_0^2 \\ &-2kH\omega_{\rm G}^2\left((C+NS)\,\omega_0^2 - (N-1)S\omega_{\rm G}^2\right), \\ \lambda_{\rm den} &= \left((1-\kappa_0)\,(C+NS) - 2kH\,(S+NC)\right)\kappa_0\omega_0^4 \\ &-2kH\omega_{\rm G}^2\left((C+NS)\,\omega_0^2 - (N-1)S\omega_{\rm G}^2\right). \end{aligned}$$

The frequency shift is linear in ω_A^2 and it also depends on the physical parameters N, H and L explicitly and, thorugh ω_0, implicitly. The linear behaviour, a posteriori, justifies our choice of the profile for the Alfvén speed.

In order to understand the analytical results, Equation (47), the dependence of the frequency shift on model parameters N, H and L can be discussed by displaying $\Delta\nu(l)$ for a series of values of each parameter. A weak magnetic field is illustrated by taking $v_{AL} = 1$ km s^{-1}.

5.2.1. N-Dependence

The drop of the plasma density right above the photosphere is another dynamically varying quantity. According to 3D simulation results in, e.g., Trampedach et al. (2014), the density drops by a factor of 30 in a layer a 1 Mm above the photosphere. In the present models above, the value for N was chosen to be 10. The influence of the density drop ratio, N, on the frequency shift due to a weak magnetic field is shown in Figure 4 for values $N = 2$, 5, 10, 100 and 1000. The other two model parameters, the thickness of the transitional layer, L, and the scale height at the top of the transitional layer, H, are fixed at $L = 2$ Mm and $H = 1.5$ Mm. These values are not necessarily considered solar representatives as they do not take fixed values in the dynamic Sun. However, taking them as parameters may give a deeper insight in the understanding of solar atmospheric oscillations.

In the low-degree range, $l \leq l_{CR}$, the shift increases steadily with increasing l up to about 0.9 μHz, reached at $l = l_{CR}$, indicated by a dotted line. For larger values of N, a significant increase in shift starts at higher harmonic degrees but it reaches the same maximum, and the value for l_{CR} does not vary noticeably with N either. A large value of N indicates a thin atmosphere, $\rho_t << \rho_i$, which explains why the f-mode frequency does not change significantly for $N = 1000$, only in a narrow range of l, near $l = l_{CR}$.

There are no f modes with harmonic degrees $l_{CR} < l < l_{RC}$. This gap decreases with increasing N, as the upper boundary of the range, l_{RC}, indicated in the plots by vertical dashed lines, is decreasing while the lower boundary, l_{CR}, is not changing significantly with N.

In the high-degree range, $l \geq l_{RC}$, the frequency shift decreases with l. This decrease is sharper for larger values of N as a thinner atmosphere has smaller influence on the properties of the f-mode oscillations. The frequency shift of the f mode for $N = 2$ is not seen in the high-degree domain in Figure 4 as the threshold value l_{RC} increases rapidly as the density drop ratio decreases to $N = 1$. For $N = 2$, $l_{RC} \approx 1350$, which is above the displayed range of harmonic degree.

5.2.2. H-Dependence

The variation of the frequency shift due to changes in the atmospheric density scale-height, H, is shown in Figure 5, where $\Delta\nu(l)$ is given for seven typical values of H between 0.5 and 10 Mm. The other two model parameters

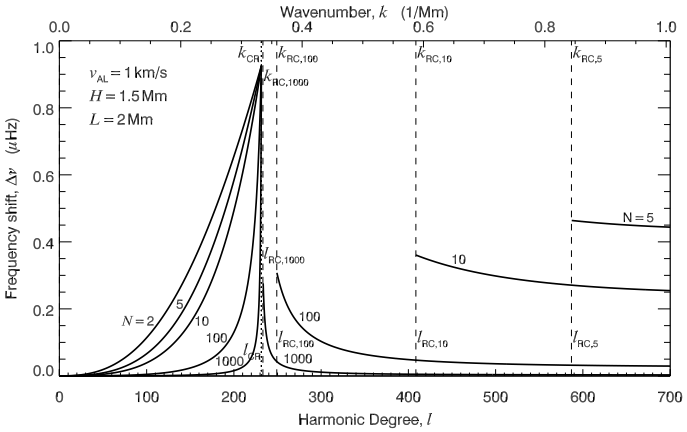

Figure 4: Shift of f-mode frequencies as a function of harmonic degree in weak-field approximation, $v_{AL} = 1$km s^{-1}, for nine values of the factor of density drop at the photosphere, between $N = 2$ and 1000. With increasing harmonic degree up to $l = l_{CR}$ (≈ 231), the frequency shifts increase towards the same value, $\Delta\nu \approx 0.92\mu$Hz. There are no f modes with harmonic degrees between l_{CR} and l_{RC}. For $l \geq l_{RC}$, the frequency shifts decrease. While l_{CR} and k_{CR} are independent of N, l_{RC} and k_{RC} increase with decreasing N. The numbers in the indices of l_{RC} and k_{RC} are N for which l_{RC} and k_{RC} take the value indicated by the vertical dashed line.

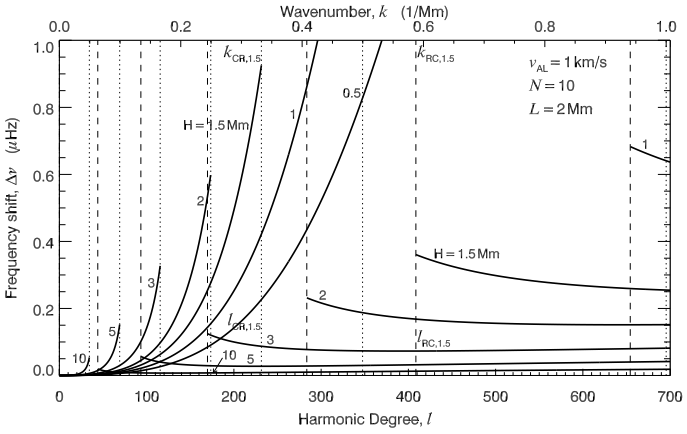

Figure 5: Shift of the f-mode frequency versus harmonic degree in weak-field approximation for seven values of the density scale-height between $H = 0.5$ and 10 Mm. With increasing harmonic degree up to $l = l_{CR}$ (vertical dotted lines), the frequency shifts increase. F modes do not exist with harmonic degrees between l_{CR} and l_{RC} (vertical dashed lines). For $l \geq l_{RC}$, the frequency shifts decrease from lower values than those taken just below l_{CR}. The characteristic harmonic degrees, l_{CR} and l_{RC}, and wavelengths, k_{CR} and k_{RC}, defined in the main text, are labeled only for $H = 1.5$.

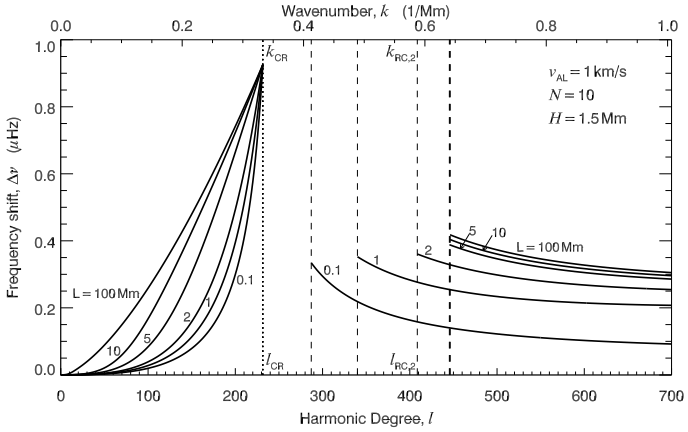

Figure 6: Shift of f-mode frequencies as a function of harmonic degree in weak-field approximation, $v_{AL} = 1\text{km s}^{-1}$, for six values of the thickness of the intermediate layer between $L = 0.1$ and 100 Mm. With increasing harmonic degree up to $l = l_{CR}$ (≈ 231), the frequency shifts increase towards the same value, $\Delta\nu \approx 0.92\mu$Hz. There are no f modes with harmonic degrees between l_{CR} and l_{RC}. For $l \geq l_{RC}$, the frequency shifts decrease. The characteristic harmonic degrees, l_{CR} and l_{RC}, and wavelengths, k_{CR} and k_{RC}, are defined in the main text. While l_{CR} and k_{CR} are independent of L, l_{RC} and k_{RC} increase with increasing L. The number 2 in the index of l_{RC} and k_{RC} indicates that those threshold values belong to the $L = 2$Mm case.

are fixed at $N = 10$ and $L = 2$ Mm. The threshold values l_{CR} and l_{RC} are labelled with vertical dotted and dashed lines, respectively, for each value of H.

For a fixed value of H, the frequency shift increases as the harmonic degree increases and takes its maximum at $l = l_{RC}$. The maximum values taken by the frequency shifts for $H = 1$ and 0.5 Mm, $\Delta\nu \approx 1.7\mu$ Hz at $l \approx 348$ and $\Delta\nu \approx 4.8\mu$ Hz at $l \approx 696$, respectively, are above the range displayed in Figure 5.

Analysing the l-dependence further, the shift takes a value at $l = l_{RC}$ and tends to zero as l increases. For larger scale-heights, the upper boundary of the low-degree domain, l_{CR} decreases and the maximum shift, taken at l_{RC} also decreases. The gap in l for unstable solutions, with no f mode, decreases with increasing H as l_{CR} decreases faster than l_{RC}. They are labelled only for $H = 1.5$ Mm.

5.2.3. L-Dependence

The frequency shift is displayed for six values of the thickness, L, of the transitional layer in Figure 6. This particular study of L-dependence is relevant because there is little known about the actual vertical extent of the solar chromosphere. For example, its extent is dependent on the phase of solar cycle, i.e. it certainly correlates with the strength of atmospheric magnetism. The other two model parameters are $N = 10$ and $H = 1.5$ Mm.

The thickness does not have any noticeable influence either on the size of the low-degree range or on the maximum shift taken at l_{RC}, as l_{RC} does not vary significantly with L. However, within the low-degree range, $l < l_{RC}$, the frequency shift is larger for larger L. In the two-layer model, where $L = 0$, the shift of the f-mode frequency in the low-degree range, given generally in Eq. (47), reduces to:

$$\Delta\nu = \frac{kH}{N - 2(N-1)kH} \frac{\nu_A^2}{\nu_G}.$$

In the high-degree range, the frequency shift of the f mode becomes:

$$\Delta\nu = \frac{\left(2(N-1)kH - N\right)^2 + N^2}{4d(N-1)\left(2(N-1)kH - N\right)} \frac{\nu_A^2}{\nu_G}$$

with

$$d \equiv \sqrt{\left((N^2-1)\,kH - N\right)kH}.$$

The lower boundary of the high-degree domain, l_{CR}, increases with increasing L, and the increase slows down and becomes insignificant from $L \approx 5$ Mm. The maximum frequency shift, taken at $l = l_{CR}$, slightly increases as L increases.

6. Thin-Layer Approximation

After exploring the behaviour of the fundamental oscillation mode in a solar environment with an atmosphere embedded in a weak magnetic field, in the following, this condition is now relaxed and there is no restriction on the atmospheric magnetic field strength. Instead, we assume that the thickness, L, of the transitional layer is much smaller than the wavelength of the studied oscillations, i.e., $L << \lambda\,(\equiv 2\pi/k)$, or:

$$kL << 1. \tag{48}$$

The presence of a thin transitional layer where the magnetic field strength increases from zero to its maximum between the photosphere, $z = 0$, and the top of the layer, $z = L$, modifies the f-mode frequency slightly:

$$\omega = \omega_0 + \Delta\omega, \tag{49}$$

where ω_0 is the mode frequency for the two-layer model, $L = 0$, and the shift due to the thin transitional layer is

$$\Delta\omega << \omega_0. \tag{50}$$

The properties of the f-mode oscillations in a thin-layer model can be studied analytically by linearising the dispersion relation, Equation (27), with respect to kL.

$$\begin{aligned} 0 = {} & \kappa\left(\omega_0^2 - \omega_A^2\right) \\ & \times \left((1-\kappa)\left(\omega_0^2 - \omega_A^2\right)\gamma^2\left(\ln\left(\omega_0^2\right) - \ln\left(\omega_0^2 - \omega_A^2\right)\right)\right. \\ & \left. -kH\omega_0^2\left(2\omega_0^2 - \omega_A^2\right)\right)kL \\ & -4kH\omega_A^2\omega_0\left(\omega_G^2 - \kappa\left(N\omega_A^2 - (N-1)\omega_G^2\right)\right)\Delta\omega. \end{aligned} \tag{51}$$

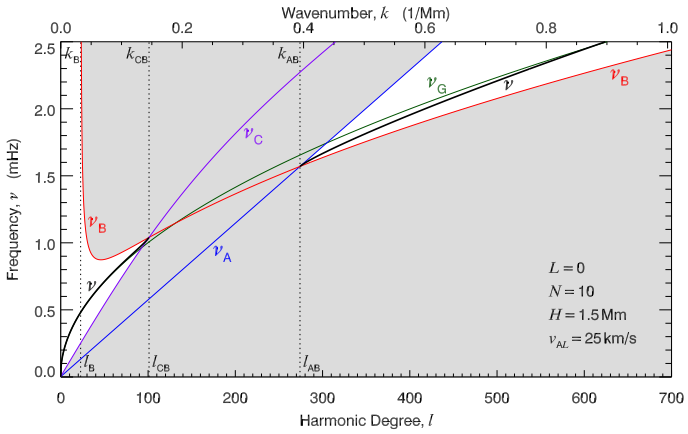

Figure 7: Frequency spectrum of the two-layer, $L = 0$, model with an atmosphere embedded in a horizontal magnetic field. The fundamental mode can have a harmonic degree either lower than $l_{\rm CB}$ or higher than $l_{\rm AB}$. The characteristic harmonic degrees, $l_{\rm B}$, $l_{\rm CB}$ and $l_{\rm AB}$, and wavelengths, $k_{\rm B}$, $k_{\rm CB}$ and $k_{\rm AB}$, are defined in the main text.

6.1. Analytical Solutions in the Two-Layer Model

The dispersion relation for a two-layer model, $L = 0$, with a magnetic atmosphere can be obtained by separating the leading terms, which contain neither $\Delta\omega$ nor kL, of the linearised, with respect to kL, dispersion relation, in Eq. (51):

$$(1 - 2NkH - \kappa)\left(\omega_0^2 - \omega_{\rm A}^2\right) = 2kH\left(N\omega_{\rm A}^2 - (N-1)\omega_{\rm G}^2\right). \tag{52}$$

The above dispersion relation can be rearranged to:

$$B\omega^2\left(\omega_0^2 - \omega_{\rm B}^2\right) = \sqrt{\left(1 + 4k^2H^2\right)\left(\omega_0^2 - \omega_{\rm C}^2\right)\left(\omega_0^2 - \omega_{\rm A}^2\right)}, \tag{53}$$

with

$$\begin{aligned} B &\equiv 1 - 2NkH, \\ \omega_{\rm B}^2 &\equiv \frac{\omega_{\rm A}^2 - 2(N-1)kH\omega_{\rm G}^2}{1 - 2NkH}. \end{aligned} \tag{54}$$

Squaring Equation (53) yields a second-order equation for ω_0^2, the solutions of which are:

$$\omega_\pm^2 = \frac{\lambda_{\rm num} \pm \sqrt{\lambda_{\rm D}}}{\lambda_{\rm den}}, \tag{55}$$

where

$$\begin{aligned} \lambda_{\rm num} &= \left(2(N-1)kH - 1\right)N\omega_{\rm G}^2 - (2kH + N)\,\omega_{\rm A}^2, \\ \lambda_{\rm den} &= 2\left(\left(N^2 - 1\right)kH - N\right), \\ \lambda_{\rm D} &= \left(1 + 4k^2H^2\right)N^2\omega_{\rm AL}^4 \\ &- 2N\left(4(N-1)k^2H^2 - 2NkH + N\right)\omega_{\rm G}^2\omega_{\rm A}^2 \\ &+ \left(2(N-1)kH - N\right)^2\omega_{\rm G}^4. \end{aligned}$$

The solutions $\omega_0^2 = \omega_+^2$ and $\omega_0^2 = \omega_-^2$ are also roots of dispersion relation (53) only if

$$\omega_0 \le \min\left(\omega_{\rm A}, \omega_{\rm C}\right) \qquad \text{or} \qquad \omega_0 \ge \max\left(\omega_{\rm A}, \omega_{\rm C}\right) \tag{56}$$

and

$$B\left(\omega_0^2 - \omega_{\rm B}^2\right)\left(\omega_0^2 - \omega_{\rm A}^2\right) > 0. \tag{57}$$

These conditions provide permitted f-mode oscillations of the model, solutions to Equation (53). Frequencies $\omega_{\rm C}$ and $\omega_{\rm B}$ and $\omega_{\rm A}$, defined by Equations (22), (54) and (18), are characteristic cut-off frequencies, which, in a frequency spectrum, separate regions of eigen-mode frequencies from regions where no real solutions to the dispersion relation can occur.

The frequency spectrum for the thin-layer approximation is shown in Figure 7 for an atmospheric magnetic field fixed at $v_{\rm AL} = 25$ km s^{-1}. Taking a density, $\rho \approx 100$ g m^{-3}, this Alfvén speed is associated with a magnetic field of the order of $B \approx 1G$, which may seem relatively weak. Note, however, that this value models the entire bottom of the chromosphere, which represents an average value, not only the field strength of magnetically active regions. The photospheric density drop is $N = 10$ and the atmospheric density scale-height is $H = 1.5$ Mm. The harmonic degree, for $l \le 700$, and the associated wavenumber, k, are shown along the lower and upper horizontal axes, respectively. As before, it is the cyclic frequencies, ν, that are given in the spectra.

The frequency regions where the conditions in Equations (56) and (57) are not satisfied are shaded grey. Three threshold values for l (and k) are indicated by dotted and dashed lines.

The characteristic frequency $\nu_{\rm B}\left(\equiv \dfrac{\omega_{\rm B}}{2\pi}\right)$ is discontinuous at $k_{\rm B} \equiv \dfrac{1}{2NH}$, indicated by a vertical dashed line, as the denominator of $\nu_{\rm B}^2$, becomes zero at that value of k. For the parameter values taken in Figure 7, $\nu_{\rm B}^2$ is negative for $k < k_{\rm B}$, hence $\nu_{\rm B}$ is imaginary, and positive for $k > k_{\rm B}$.

Frequencies $\nu_{\rm C}$ and $\nu_{\rm B}$ are equal at $k = k_{\rm CB}$ and frequencies $\nu_{\rm A}$ and $\nu_{\rm B}$ are equal at $k = k_{\rm CB}$. In the range $0 \le k \le k_{\rm B}$ for $\nu > \nu_{\rm C}$, while in the range $k_{\rm B} < k \le k_{\rm CB}$ for $\nu_{\rm C} < \nu < \nu_{\rm B}$, solutions to the quadratic equation, also satisfy the dispersion relation, Equation (53), as the eigen-frequency values satisfy the conditions (56) and (57). The interval $0 \le k \le k_{\rm CB}$ is the small-wavenumber or low-degree range of f modes. There is no permitted region for eigen-frequencies in the range $k_{\rm CB} < k < k_{\rm AB}$. This range is a gap, f-mode oscillations cannot exist with wavenumbers falling within this interval.

Out of the two solutions, given by Equation (55), it is ν_+ that is above $\nu_{\rm C}$, and below $\nu_{\rm B}$ where $\nu_{\rm B}$ exists, in the low-l region. At $l = 0$, $\nu = 0$. For $l > 0$, the f-mode frequency is slightly larger than $\nu_{\rm G}$. The difference is noticeable only at $l \approx l_{\rm CB}$.

The semi-infinite interval $k \ge k_{\rm AB}$ is the large-wavenumber or high-degree range of f modes. In the high-degree range, it is ν_- that satisfies the dispersion relation, Equation (53). Its value is lower than $\nu_{\rm G}$, however, the difference tends to zero as l increases.

Using Eq. 1, the threshold wavenumbers can be converted to threshold harmonic degrees: $l_{\rm B} = k_{\rm B}R_{\rm Sun}$, $l_{\rm CB} =$

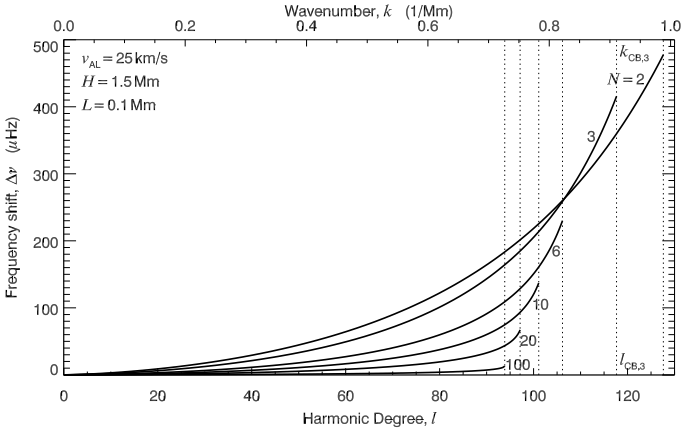

Figure 8: Shift of f-mode frequencies as a function of harmonic degree in thin-layer approximation, $L = 0.1$Mm, for six values of the density ratio between $N = 2$ and 100. With increasing harmonic degree up to $l = l_{\rm CB}$, the frequency shifts increase, where the f mode terminates. Number 3 in the index of $l_{\rm CB}$ and $k_{\rm CB}$ indicates that those threshold values belong to the $N = 3$ case.

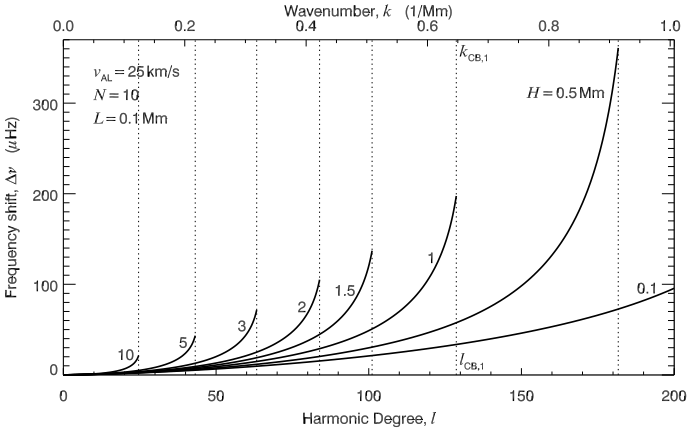

Figure 9: Shift of f-mode frequencies as a function of harmonic degree in thin-layer approximation, $L = 0.1$Mm, for eight values of the atmospheric density scale-height between $H = 0.1$ and 10 Mm. With increasing harmonic degree up to $l = l_{{\rm CB},H}$, the frequency shifts increase, where the f mode terminates. Number 1 in the index of $l_{\rm CB}$ and $k_{\rm CB}$ indicates that those threshold values belong to the $L = 1$ Mm case.

$k_{\rm CB}R_{\rm Sun}$, and $l_{\rm AB} = k_{\rm AB}R_{\rm Sun}$.
The solutions ω_- and ω_+ are called the low- and high-degree solutions.

6.2. Analytical Solutions to the Thin-Layer Approximation

The first-order terms of the dispersion relation, linearised with respect to kL, Eq. (51), provide the factor between the thickness of the transitional layer, L, and the resulting frequency shift:

$$\Delta\omega = \left((1-\kappa)\left(\omega_0^2-\omega_{\rm A}^2\right)\gamma^2\left(\ln\omega_0^2-\ln\omega_0^2-\omega_{\rm A}^2\right)\right.$$
$$\left.-kH\omega_{\rm A}^2\left(2\omega_0^2-\omega_{\rm A}^2\right)\right)$$
$$\times\frac{\kappa\left(\omega_0^2-\omega_{\rm A}^2\right)}{4kH\omega_{\rm A}^2\left(\omega_{\rm G}^2-\kappa\left(N\omega_{\rm A}^2-(N-1)\omega_{\rm G}^2\right)\right)}\frac{kL}{\omega_0}. \quad (58)$$

Although the dependence of the frequency shift is linear with L, it is rather complicated on the other parameters, N, H, and $v_{{\rm A}L}$.

Recall that the f-mode frequency in the low-degree range, $l \geq l_{\rm CB}$, is $\omega_0 = \omega_+$. Hence, ω_0 has to be replaced in Equation (58) by ω_+, given by Equation (55). $\Delta\omega$ is a function of the frequency of the two-layer model, ω_0, explicitly and, through κ and γ, implicitly.

In the high-degree range, $l \geq l_{\rm AB}$, the two-layer solution is $\omega_0 = \omega_-$, given by Equation (55), which is lower than $\omega_{\rm A}$. In a solar atmosphere model with a transitional layer between $z = 0$ and L, regardless of how small L is, the Alfvén frequency increases continuously from zero to $\omega_{\rm A}$ as the height increases from $z = 0$ to L. Consequently, there is always a certain height, $z = z_{\rm r}$, where the local value of the Alfvén frequency, $v_{\rm A}(z_{\rm r})$, equals the global frequency of the f-mode oscillation, ν_-. At that particular height, the local Alfvén wave, which propagates parallel to the horizontal magnetic field line, will be coupled resonantly to the global f mode oscillation. This coupling is resonant as the dispersion relation, Equation (27) is singular at $z = z_{\rm r}$ because the Bessel functions $K_0\left(\zeta(z)\right)$ and $K_1\left(\zeta(z)\right)$ are singular at $z = z_{\rm r}$ as $\zeta(z_{\rm r}) = 0$. Physically, near the resonant height, the oscillation amplitudes of the f mode increase so much that dissipative effects cannot be neglected anymore when describing the mechanism of wave propagation. Therefore, in order to find the frequency shift of the f mode oscillations with high harmonic degrees, $l \geq l_{\rm AB}$, the full dissipative MHD equations have to be solved. In a follow-up work, it will be shown that the dissipative equations can be solved analytically by using well-justified simplifications.

Our model parameters, such as N, H or $v_{{\rm A}L}$, do not have well constrained values in the solar model. For this reason, the shift of the cyclic frequency, $\Delta\nu$, due to the presence of a thin, say $L = 0.1$ Mm, transitional layer at the bottom of the atmosphere in the low-degree range, $l \leq l_{\rm CB}$, is shown in Figures 8 to 10 for a set of values for N, H and $v_{{\rm A}L}$, respectively, while the other model parameters are fixed at $N = 10$, $H = 1.5$ Mm and $v_{{\rm A}L} = 25$ km s^{-1}. The upper boundary of the low-degree range is the threshold value $l = l_{\rm CB}$, which is indicated by vertical dotted lines for each parameter value.

The frequency shift, below 200 μHz and typically a few tens of μHz, is significantly wider range than found in the weak-field model. This predicts strong influence of atmospheric magnetic fields on f modes. With an increase of N, H or $v_{{\rm A}L}$, $l_{\rm CB}$ decreases, which reduces the l range of the f mode. As the harmonic degree increases from $l = 0$ to $l_{\rm CB}$, the frequency shift increases from zero to a maximum value. The maximum value, taken at $l_{\rm CB}$, is larger for larger N and H and for smaller $v_{{\rm A}L}$.

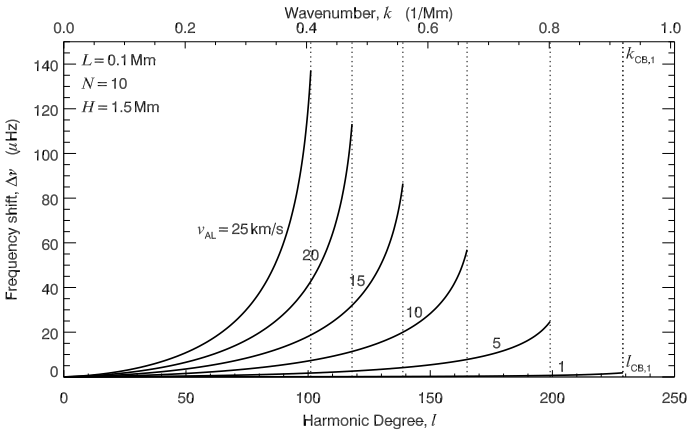

Figure 10: Shift of the f-mode frequency versus harmonic degree in thin-layer approximation for six values of the characteristic Alfvén speed between $v_{AL} = 1$ and 25 km s^{-1}. With increasing harmonic degree up to $l = l_{CB}$, the frequency shifts increase, where the f mode terminates. Number 1 in the index of l_{CB} and k_{CB} indicates that those threshold values belong to the $L = 1$ Mm case.

7. Summary and Conclusion

The effects of a magnetic atmosphere on the fundamental (f) oscillation mode of the solar interior is studied here in an incompressible medium. A three-layer slab geometry approximation seems to be adequate for progress to determine the atmospheric frequency shifts of the f mode. The shifts were derived analytically, using realistic approximations. The model proposed and investigated here consists of a semi-infinite interior layer, a semi-infinite magnetic atmospheric layer and a transitional layer of finite width between them, where the strength of a horizontal magnetic field increases continuously with height from zero to its atmospheric maximum.

The general dispersion relation, $f(\omega, k)$ has been derived and solved analytically for three distinct cases: a two-layer, a weak-field and a thin-layer approximation. A set of f-mode frequencies has been found in a low-degree range and another set in a high-degree range. A window between the low- and high degree ranges has also been identified for which no f mode oscillations are permitted. This is one of the consequences of the presence of the atmosphere as without it, there are no windows in the frequency spectrum with no f modes. The boundaries between the low-l interval, the window without any f mode and the semi-infinite high-l interval are threshold harmonic degrees defined by characteristic frequencies of the model.

In the two- and three-layer models with no atmospheric magnetic field, the frequency of the f mode in the low-l domain equals the fundamental frequency, $\omega = \omega_G$, which is the fundamental mode frequency in a model of the solar interior with no atmosphere (Christensen-Dalsgaard, 2002). In the high-l domain, this value is reduced by the presence of an atmosphere in the range of ten to twenty per cent. However, this reduction tends to zero in a magnetic atmosphere as $\lim_{k\to\infty} \omega_- = \omega_G$.

The present paper focusses on the frequency spectrum of global oscillations. The spatial aspect of the f modes, i.e., how the radial profile of perturbations are modified by atmospheric changes, should be the subject of another study.

Windows with no real f- and/or p-mode frequencies in the eigen-frequency spectrum have been found in several numerical studies of solar atmospheric models (e.g., Campbell & Roberts, 1989; Pintér & Goossens, 1999; Vanlommel & Goossens, 1997; Pintér et al., 2007). The nature of f-mode oscillations is confirmed by the analytical study. Our simple model proposed also predicts that the boundaries of the domains of non-propagating solutions are sensitive to the equilibrium parameters. Complex oscillation frequencies arising from algebraic equations of simple models indicate finite lifetime of the modelled oscillation modes. Global oscillations with real frequency in these models do not decay in time. In reality, however, there are various reasons, such as dissipative effects, that make the lifetime of all oscillation modes finite. Therefore, we should not expect clear non-propagation gaps in eigen-frequency spectra based on helioseismic observations, as all the quantities, that have fixed values in the numerical or analytical models, are continuously changing in the interior and atmosphere of the dynamic Sun. Another reason for not finding non-propagating windows for f-modes in observations can be that, as the present model predicts, the larger the density drop (N) at the photosphere, the narrower the l-range where f-modes cannot exist. A decisive experiment that could test the existence of oscillation-free windows in the solar spectrum would require observations of higher temporal resolution than those currently available from BiSON, SOHO/MDI, or SDO/HMI. One approach of such a test could be the observation of selected oscillation modes at times of solar minimum only or at active regions with a fixed magnetic field strength, by which a large-range variation of plasma parameters could be avoided.

The equilibrium model used in this investigation has a simplified structure, mainly in order to gain insight by analytical calculations. Each region of the Sun approximated here, including the interior, the photosphere and the atmosphere, is far more complex than suggested. One of the strongest simplifications in the model is the magnetic field. The intricate structure of the solar atmospheric magnetic field is reduced to a global horizontal field of which the characteristic strength varies only vertically. The profile and the thickness of the layer where the kinetic pressure and the magnetic field strength varies continuously in the lower solar atmosphere also varies dynamically in space, which is fully omitted from the model. Obviously, it is not the main aim of this study to reproduce all the fine details of observational results. The purpose of the present analytical derivations is to gain a fully parametrised insight into general tendencies in the way how the solar interior and the lower atmospheric wave fields are coupled to each other. By this reductionist approach, we showed that a magnetic atmosphere plays a significant role and, e.g., can

indeed be accounted for the shift of the eigen-frequency of helioseismic f modes by the order of the observed amount.

Last but not least, let us recall that an important phenomenon for the coupling between the solar interior and magnetic atmosphere is resonance. Resonance occurs at regions where the local frequency of an MHD wave (Alfvén or slow oscillation) matches the global frequency of a helioseismic (f- or p-mode) oscillation. The plasma environment can provide the energy for the amplitude increase of the oscillations. The real challenge is now to investigate resonant coupling.

However, it would be obstructive to embark on such studies without a clear and much simpler insight into the current non-resonant model. Not to mention, having such investigation in the same paper may be too elaborate and lengthy.

In the solar interior, f- and p-mode oscillations exist. The present model, with uniform density distribution in the interior and an incompressible plasma, describes only f modes. For an investigation of the p-mode properties, compressibility has to be allowed for, and the constant density in the interior should be replaced by a polytrope. Similarly, internal and atmospheric gravity oscillation modes (Christensen-Dalsgaard, 2002; Pintér, 2008) are also missing from the analysis, as the Brunt-Väisälä frequency is zero in the interior and transitional layer and its square is negative in the atmosphere. A further understanding of the mechanisms how p modes are effected by the lower atmosphere and also the intense search for solar gravity waves, which could reveal still unknown properties of the solar core, demands another investigation of the frequency spectrum of an enhanced model with a compressible environment.

8. Acknowledgement

BP is thankful to his family for their support, and acknowledges the hospitality received by MSRC Visitor Grant Programme of Sheffield University (UK). RE is grateful to STFC (UK), The Royal Society and the Chinese Academy of Sciences President's International Fellowship Initiative Nr. 2016VMA045 for support received.

9. References

Abramowitz, M. & Stegun, I. A. 1970, Handbook of mathematical functions with formulas, graphs, and mathematical tables, Dover Publications, Inc., New York, 374-377

Antia, H. M., Basu, S., Pintar, J., & Pohl, B. 2000, Solar Cycle Variation in Solar f-Mode Frequencies and Radius, *Solar Phys.*, 192, 459-468

Cally, P. S. & Bogdan, T. J. 1993, Solar p-modes in a vertical magnetic field - Trapped and damped pi-modes, *The Astrophys. J.*, 402, 721-732

Cally, P. S., Bogdan, T. J., & Zweibel, E. G. 1994, Umbral oscillations in sunspots: Absorption of p-modes and active region heating by mode conversion, *The Astrophys. J.*, 437, 505-521

Campbell, W. R. & Roberts, B. 1989, The influence of a chromospheric magnetic field on the solar p- and f-modes, *The Astrophys. J.*, 338, 538-556

Tripathy, S. C., Hill, F., Jain, K., & Leibacher, J. W. 2006, Changes to global mode parameters over a solar cycle, *Mon. Not. R. Astron. Soc.*, 624, 32-42

Chaplin, W. J., Elsworth, Y., Isaak, G. R., Miller, B. A., & New, R. 2004, The solar cycle as seen by low-l p-mode frequencies: comparison with global and decomposed activity proxies, *Mon. Not. R. Astron. Soc.*, 352, 1102-1108

Chaplin, W. J., Elsworth, Y., Miller, B. A., Verner, G. A., & New, R. 2007, Solar p-Mode Frequencies over Three Solar Cycles, *The Astrophys. J.*, 659, 1749-1760

Christensen-Dalsgaard, J. 2002, Helioseismology, Reviews of Modern Physics, 74, 1073-1129

Christensen-Dalsgaard, J., Di Mauro, M. P., Schlattl, H., & Weiss, A. 2005, On helioseismic tests of basic physics, *Mon. Not. R. Astron. Soc.*, 356, 587-595

Dziembowski, W. A., & Goode, P. R. 2005, Sources of Oscillation Frequency Increase with Rising Solar Activity, *The Astrophys. J.*, 625, 548-555

Elsworth, Y., Howe, R., Isaak, G. R., McLeod, C. P., Miller, B. A., New, R., & Wheeler, S. J. 1995, Techniques used in the analysis of solar oscillations data from the BiSON (University of Birmingham) network. I. Daily calibration., *Astron. Astrophys. Suppl.*, 113, 379-386

Erdélyi, R. 2006, Magnetic coupling of waves and oscillations in the lower solar atmosphere: can the tail wag the dog?, Royal Society of London Philosophical Transactions Series A, 364, 351-381

Erdélyi, R. 2006, Magnetic seismology of the lower solar atmosphere, Royal Society of London Philosophical Transactions Series A, 624, 15.1-13

Erdélyi, R., Kerekes, A., & Mole, N. 2005, Influence of random magnetic field on solar global oscillations: The incompressible f-mode, *Astron. Astrophys.*, 431, 1083-1088

Erdélyi, R., Hague, A., & Nelson, C. J. 2014, Effects of Stratification and Flows on P $_1$/ P $_2$ Ratios and Anti-node Shifts Within Closed Loop Structures, *Solar Phys.*, 289, 167-182

Giovanelli, R. G. 1980, An exploratory two-dimensional study of the coarse structure of network magnetic fields, *Solar Phys.*, 68, 49-69

Hindman, B. W., Zweibel, E. G., & Cally, P. S. 1996, Driven Acoustic Oscillations within a Vertical Magnetic Field, *The Astrophys. J.*, 459, 760-772

Ishikawa, R., Tsuneta, S., & Jurčák, J. 2010, Three-Dimensional View of Transient Horizontal Magnetic Fields in the Photosphere, *The Astrophys. J.*, 713, 1310-1321

Ishikawa, R., & Tsuneta, S. 2010, Spatial and Temporal Distributions of Transient Horizontal Magnetic Fields with Deep Exposure, *The Astrophys. J. Lett.*, 718, L171-175

Jefferies, S. M., Duvall, Jr., T. L., Harvey, J. W., & Pomerantz, M. A. 1990, Helioseismology from the South Pole: Results from the 1987 Campaign, *Solar Phys.*, 367, 135-143

Kerekes, A., Erdélyi, R., & Mole, N. 2008, A Novel Approach to the Solar Interior-Atmosphere Eigenvalue Problem, *The Astrophys. J.*, 683, 527-535

Kerekes, A., Erdélyi, R., & Mole, N. 2008, Effects of Random Flows on the Solar f Mode: II. Horizontal and Vertical Flow, *Solar Phys.*, 251, 469-489

Lamb, H. 1932, Hydrodynamics, *The Astrophys. J.*, 531, 1094-1108

Liang, Z.-C., Gizon, L., Schunker, H., & Philippe, T. 2013, Helioseismology of sunspots: defocusing, folding, and healing of wavefronts, *Astron. Astrophys.*, 558, A129.1-4

Libbrecht, K. G., & Woodard, M. F. 1990, Solar-cycle effects on solar oscillation frequencies, *Nature*, 345, 779-782

Lites, B. W., Kubo, M., Socas-Navarro, H., Berger, T., Frank, Z., Shine, R., Tarbell, T., Title, A., Ichimoto, K., Katsukawa, Y., Tsuneta, S., Suematsu, Y., Shimizu, T., & Nagata, S. 2008, The Horizontal Magnetic Flux of the Quiet-Sun Internetwork as Observed with the Hinode Spectro-Polarimeter, *The Astrophys. J.*, 672, 1237-1253

Mather, J. F., & Erdélyi, R. 2016, Magneto-Acoustic Waves in a Gravitationally Stratified Magnetized Plasma: Eigen-Solutions and their Applications to the Solar Atmosphere, *The Astrophys. J.*, 822, 116-130

Mole, N., Kerekes, A., & Erdélyi, R. 2008, Effects of Random Flows on the Solar f Mode: I. Horizontal Flow, *Solar Phys.*, 251, 453-468
Pintér, B., & Erdélyi, R. 2011, Effects of Magnetic Fields in the Solar Atmosphere on Global Oscillations, *Space Sci. Rev.*, 158, 471-504
Pintér, B. 2008, Modelling solar atmospheric gravity oscillation modes, Astronomische Nachrichten, 329, 503-507
Pintér, B. 2008, Modelling the Coupling Role of Magnetic Fields in Helioseismology, *Solar Phys.*, 251, 329-340
Pintér, B. 1999, The influence of the atmospheric magnetic field on solar oscillation modes, Katholieke Universiteit Leuven, Belgium
Pintér, B., Erdélyi, R., & Goossens, M. 2007, Global oscillations in a magnetic solar model. II. Oblique propagation, *Astron. Astrophys.*, 466, 377-388
Pintér, B., & Goossens, M. 1999, Oscillations in a magnetic solar model. I. Parallel propagation in a chromospheric and coronal magnetic field with constant Alfvén speed, *Astron. Astrophys.*, 347, 321-334
Sakurai, T., Goossens, M., & Hollweg, J. V. 1991, Resonant behaviour of MHD waves on magnetic flux tubes. I - Connection formulae at the resonant surfaces., *Solar Phys.*, 133, 227-245
Spruit, H. C., & Bogdan, T. J. 1992, The conversion of p-modes to slow modes and the absorption of acoustic waves by sunspots, *The Astrophys. J. Lett.*, 391, L109-112
Taroyan, Y. 2004, MHD waves and instabilities in steady states, The University of Sheffield
Taroyan, Y., & Erdélyi, R. 2008, Global Acoustic Resonance in a Stratified Solar Atmosphere, *Solar Phys.*, 251, 523-531
Taroyan, Y. & Erdélyi, R. 2008, Resonant acoustic waves in a stratified atmosphere, Proceedings of the International Astronomical Union, IAU Symposium, 247, 86-89
Taroyan, Y., Erdélyi, R., & Doyle, J. G. 2004, Time-Distance Helioseismology and the Magnetic Atmosphere of the Sun, SOHO 13 - Waves, Oscillations and Small-Scale Transient Events in the Solar Atmosphere: A Joint View from SOHO and TRACE', ESA Special Publication, 547, 33-38
Thompson, M. J. 2006, Magnetohelioseismology, Royal Society of London Philosophical Transactions Series A, 364, 297-311
Tirry, W. J., Goossens, M., Pintér, B., Čadež, V., & Vanlommel, P. 1998, Resonant Damping of Solar p-Modes by the Chromospheric Magnetic Field, *The Astrophys. J.*, 503, 422-428
Trampedach, R., Stein, R. F., Christensen-Dalsgaard, J., Nordlund, Å., & Asplund, M. 2014, Improvements to stellar structure models, based on a grid of 3D convection simulations - II. Calibrating the mixing-length formulation, *Mon. Not. R. Astron. Soc.*, 445, 4366-4384
Tripathy, S. C., Hill, F., Jain, K., & Leibacher, J. W. 2006, Changes to global mode parameters over a solar cycle, Proceedings of SOHO 18/GONG 2006/HELAS I, Beyond the Spherical Sun, ESA Special Publication, 624, 93.1-7
Tsuneta, S., Ichimoto, K., Katsukawa, Y., Nagata, S., Otsubo, M., Shimizu, T., Suematsu, Y., Nakagiri, M., Noguchi, M., Tarbell, T., Title, A., Shine, R., Rosenberg, W., Hoffmann, C., Jurcevich, B., Kushner, G., Levay, M., Lites, B., Elmore, D., Matsushita, T., Kawaguchi, N., Saito, H., Mikami, I., Hill, L. D., & Owens, J. K. 2008, The Solar Optical Telescope for the Hinode Mission: An Overview, *Solar Phys.*, 249, 167-196
Vanlommel, P., & Čadež, V. M. 1998, Influence of temperature profile on solar acoustic modes, *Solar Phys.*, 182, 263-281
Vanlommel, P., & Goossens, M. 1997, Influence of a chromospheric magnetic field on solar acoustic modes, *Solar Phys.*, 187, 357-387
Zhao, H., & Chou, D.-Y. 2016, Measurements of the Absorption and Scattering Cross Sections for the Interaction of Solar Acoustic Waves with Sunspots, *The Astrophys. J.*, 822, 23-35
Zhukov, V. I. 1997, Resonant absorption and the spectrum of 5-min oscillations of the Sun., *Astron. Astrophys.*, 322, 302-306
Zhugzhda, I. D., & Dzhalilov, N. S. 1982, Transformation of magnetogravitational waves in the solar atmosphere, *Astron. Astrophys.*, 112, 16-23